Impacts of increasing anthropogenic soluble iron and nitrogen deposition on ocean biogeochemistry

Aparna Krishnamurthy,[1] J. Keith Moore,[1] Natalie Mahowald,[2] Chao Luo,[2] Scott C. Doney,[3] Keith Lindsay,[4] and Charles S. Zender[1]

Received 8 December 2008; revised 29 April 2009; accepted 13 May 2009; published 28 August 2009.

[1] We present results from transient sensitivity studies with the Biogeochemical Elemental Cycling (BEC) ocean model to increasing anthropogenic atmospheric inorganic nitrogen (N) and soluble iron (Fe) deposition over the industrial era. Elevated N deposition results from fossil fuel combustion and agriculture, and elevated soluble Fe deposition results from increased atmospheric processing in the presence of anthropogenic pollutants and soluble Fe from combustion sources. Simulations with increasing Fe and increasing Fe and N inputs raised simulated marine nitrogen fixation, with the majority of the increase in the subtropical North and South Pacific, and raised primary production and export in the high-nutrient low-chlorophyll (HNLC) regions. Increasing N inputs alone elevated small phytoplankton and diatom production, resulting in increased phosphorus (P) and Fe limitation for diazotrophs, hence reducing nitrogen fixation (~6%). Globally, the simulated primary production, sinking particulate organic carbon (POC) export. and atmospheric CO_2 uptake were highest under combined increase in Fe and N inputs compared to preindustrial control. Our results suggest that increasing combustion iron sources and aerosol Fe solubility along with atmospheric anthropogenic nitrogen deposition are perturbing marine biogeochemical cycling and could partially explain the observed trend toward increased P limitation at station ALOHA in the subtropical North Pacific. Excess inorganic nitrogen ($[NO_3^-] + [NH_4^+] - 16[PO_4^{3-}]$) distributions may offer useful insights for understanding changing ocean circulation and biogeochemistry.

Citation: Krishnamurthy, A., J. K. Moore, N. Mahowald, C. Luo, S. C. Doney, K. Lindsay, and C. S. Zender (2009), Impacts of increasing anthropogenic soluble iron and nitrogen deposition on ocean biogeochemistry, *Global Biogeochem. Cycles*, *23*, GB3016, doi:10.1029/2008GB003440.

1. Introduction

[2] Atmospheric deposition of macronutrients and micronutrients set important controls on marine ecology and biogeochemistry. Atmospheric fluxes are changing with time because of climate and human influences, and contemporary patterns of marine biogeochemistry may reflect to some degree variations in atmospheric input of nutrients with time. Ongoing anthropogenic influences have particularly changed biogeochemical cycling of the nutrients, iron, and nitrogen. Modeling studies suggest that changes in climate and land use practices over recent decades may have altered dust fluxes and thus aeolian Fe inputs to open ocean regions [*Mahowald and Luo*, 2003; *IPCC*, 2001]. Humans have substantially altered the global N cycle because of increased fossil fuel combustion and agriculture [*Galloway et al.*, 2004, and references therein].

[3] The past 2 decades of research in marine sciences have established the key role played by iron in driving oceanic primary production [*Martin*, 1990; *Coale et al.*, 1996; *Falkowski et al.*, 1998; *Jickells et al.*, 2005]. Numerous studies suggest that the micronutrient iron is responsible for limiting phytoplankton productivity in the Southern Ocean, eastern equatorial Pacific, and the subarctic Pacific; these areas are characterized as high-nutrient low-chlorophyll (HNLC) regions [*Boyd et al.*, 2000; *Coale et al.*, 1996; *Boyd et al.*, 2004]. *Cassar et al.* [2007] stated that aeolian iron additions resulted in enhanced export production in the Southern Ocean and increased gross primary production over a large area of the Southern Ocean downwind of dry continental areas. *Boyd and Mackie* [2008] argued that the simulated iron deposition data set used by *Cassar et al.* [2007] was primarily derived from observations in the Northern Hemisphere; hence, their correlation estimates between export production and aeolian iron inputs in the Southern Ocean may be biased. In the subtropical

[1]Earth System Science, University of California, Irvine, California, USA.
[2]Earth and Atmospheric Sciences, Cornell University, Ithaca, New York, USA.
[3]Department of Marine Chemistry and Geochemistry, Woods Hole Oceanographic Institution, Woods Hole, Massachusetts, USA.
[4]Climate and Global Dynamics Division, National Center for Atmospheric Research, Boulder, Colorado, USA.

0886-6236/09/2008GB003440$12.00

regions, diazotrophs (nitrogen fixers) may be limited by iron [*Falkowski*, 1997; *Michaels et al.*, 2001; *Berman-Frank et al.*, 2001; *Moore et al.*, 2004, 2006], and this iron requirement for nitrogen fixation may give the subtropics and tropics a sensitivity to atmospheric dust (iron) inputs similar to that seen in the HNLC regions [*Michaels et al.*, 2001; *Gruber*, 2004]. The increased biological export as a result of iron inputs to these regions leads to enhanced atmospheric CO_2 uptake [*Moore et al.*, 2006; *Boyd et al.*, 2007, and references therein]. This can have important implications for the global carbon cycle.

[4] In order to be utilized by marine phytoplankton, however, atmospheric iron deposited to the surface ocean must be in a bioavailable form. Although bioavailable iron may differ from soluble iron, we follow previous studies [e.g., *Jickells and Spokes*, 2001; *Mahowald et al.*, 2005; *Luo et al.*, 2008] and assume that soluble iron in the ferrous form is bioavailable. Much of the dissolved iron in seawater is present in colloidal forms [*Moore and Braucher*, 2008, and references therein]. Recent studies suggest that most of the soluble iron in surface waters derived from aerosols were bound to colloids [*Wu et al.*, 2007; *Aguilar-Islas et al.*, 2009]. In our model simulations we assumed a single "dissolved" seawater iron pool that is fully bioavailable, with no distinction between truly dissolved and colloidal forms. Solubility depends on the oxidation state of iron and mineralogy and this affects the biogeochemical processes involving iron in the ocean [*Luo et al.*, 2005]. Observational estimates of solubility of iron in desert soils found in an earlier study were $\sim$0.4 $\pm$ 0.3% [*Zhuang et al.*, 1992]. Solubility of iron in aerosols, however, has been found to be much higher, suggesting the importance of atmospheric processing [*Zhuang et al.*, 1992; *Pehkonen et al.*, 1993; *Siefert et al.*, 1994; *Spokes et al.*, 1994; *Desboeufs et al.*, 2001; *Hand et al.*, 2004; *Luo et al.*, 2005; *Sedwick et al.*, 2005; *Mahowald et al.*, 2005; *Fan et al.*, 2006; *Schroth et al.*, 2009].

[5] A variety of chemical processes may be relevant to iron solubility. Iron solubility is defined as the labile Fe^{2+} and Fe^{3+} fraction of total Fe and is roughly twice as large as the Fe^{2+} fraction [*Luo et al.*, 2005]. Here we consider the Fe^{2+} fraction as soluble and thus bioavailable [*Luo et al.*, 2008]. We assume that all of the soluble fraction dissolves instantaneously at the surface ocean, with some further iron release though a slower dissolution/disaggregation in the water column [*Moore et al.*, 2004]. *Luo et al.* [2005] concluded from atmospheric simulations that incorporating cloud processing (acidity of cloud droplets converts insoluble Fe into soluble Fe) and hematite (hematite in dust is a source of soluble iron) improved model-predicted iron solubility relative to observations. They also found that estimated aerosol iron solubility from the combined cloud and hematite processing case compared better with observations than other mixed processes. *Luo et al.* [2008] modified the rate coefficients in the cloud processing method from *Luo et al.* [2005] such that soluble iron values better matched observations, and the modified cloud processing method was combined with hematite reactions [*Meskhidze et al.*, 2005] to estimate soluble iron inputs to marine surface waters from aerosol deposition. The solubility estimates of *Luo et al.* [2008] are consistent with observations by *Siefert et al.* [1999], *Johansen et al.* [2000], and *Baker et al.* [2006] that fine-mode (<3 μm in diameter) iron solubility is higher than coarse-mode (>3 μm in diameter) solubility. Additionally, there is some tendency for the largest solubilities to occur far from the source areas (e.g., western tropical Atlantic and midlatitude North and South Atlantic), consistent with atmospheric processing of the iron.

[6] In addition to mineral dust, combustion may also be a source of significant soluble iron input to the ocean surface [*Siefert et al.*, 1997; *Chen and Siefert*, 2004; *Chuang et al.*, 2005, *Guieu et al.*, 2005, *Sedwick et al.*, 2007]. Combustion sources of soluble iron can be important in regions where coal combustion from power plants and industry dominate. Biofuel and biomass burning, predominantly in the tropics, could also be an important source of new iron to the ocean [*Guieu et al.*, 2005]. Iron solubility is expected to be higher in regions dominated by combustion iron because the iron is not bound in mineral form [*Schroth et al.*, 2009].

[7] Human activities, therefore, may alter the input of bioavailable iron to the surface ocean either directly through combustion iron sources or indirectly through reactive nitrogen and sulfur emissions, which subsequently result in enhanced atmospheric acidity and cloud processing. *Luo et al.* [2008] used the limited observations of iron solubility and model simulations to argue that large increases in soluble iron input to the ocean since preindustrial times are plausible, and here we explore the impact of these predicted changes on ocean biogeochemistry.

[8] Iron solubility in many previous ocean biogeochemical simulations has been assumed to be spatially constant. *Fung et al.* [2000] modeled the global distributions of annual iron uptake by phytoplankton using constant soluble iron fractions of 1% and 10% as upper and lower bounds. *Aumont et al.* [2003] and *Gregg et al.* [2003] prescribed a surface solubility of 1% in their simulations. On the basis of sensitivities studies with a box model, *Parekh et al.* [2005] set the solubility to be 1% in their simulations. Iron solubility in the BEC model has been set to a constant 2% in past studies [*Moore et al.*, 2004, 2006]. In reality, solubility of aerosol iron over global oceans is not constant [*Mahowald et al.*, 2005, and references therein], and studying the effects of varying solubility iron on ocean ecosystems is a crucial step toward understanding its role as a limiting micronutrient in many regions.

[9] Increasing fossil fuel combustion and agriculture are substantially altering the global N cycle. Atmospheric emissions of reactive nitrogen are dominated by oxidized species of nitrogen (NO_x). The net global NO_x emissions have increased from an estimated preindustrial value of 12 Tg N/a [*Holland et al.*, 1999; *Galloway et al.*, 2004] to between 42 and 47 Tg N/a in 2000. *Lamarque et al.* [2005a] forecast NO_x emissions to be 105 to 131 Tg N/a by 2100. There has been an increase since preindustrial times in the intensity of agricultural nitrogen cycling, the primary source of NH_3 emissions [*Bouwman et al.*, 2002]. Total global NH_3 emissions have increased from an estimated preindustrial value of 11 Tg N/a to 54 TgN/a for 2000 [*Holland et al.*, 1999; *Galloway et al.*, 2004] and are projected to increase to 116 Tg N/a by 2050 [*Galloway et al.*, 2004]. The spatial

patterns of atmospheric nitrogen loading to global oceans have also been impacted by anthropogenic activities [*Duce et al.*, 2008].

[10] *Doney et al.* [2007] estimated the impact of anthropogenic nitrogen (and sulfur) deposition on ocean acidification and the inorganic carbon system. They found that, on a global scale, oceanic uptake of CO_2 due to deposition of anthropogenic nitrogen resulted in an increase in the surface-dissolved inorganic carbon (DIC) and alkalinity, and a few percent increase in ocean acidification relative to that caused by anthropogenic carbon dioxide. They suggest that resulting ocean acidification could have significant effects on marine ecosystems on regional scales, especially in coastal waters downwind of industrial sources that in turn could impact human societies. *Luo et al.* [2007] used an inorganic aerosol thermodynamic equilibrium model coupled to a three-dimensional chemical transport model to understand the roles of ammonia chemistry and natural aerosols on the global distribution of NO_3^-, NH_4^+, SO_4^{2-}, dust, and sea-salt aerosols. The thermodynamic model partitions the gas-phase precursors among simulated aerosol species on the basis of relative humidity and natural and anthropogenic aerosols present. Their study concluded that, globally, atmospheric NO_3^- and NH_4^+ deposition during the 1990s was double the preindustrial deposition.

[11] In an earlier study, *Krishnamurthy et al.* [2007a] modeled the effects of atmospheric nitrogen deposition on ocean biogeochemistry using simulated atmospheric inorganic N inputs (NO_3^-, and NH_4^+) from *Luo et al.* [2007]. Inorganic nitrogen inputs from three different periods, namely, preindustrial, current, and an IPCC-A1FI prediction for 2100, were used. The IPCC-A1FI is a fossil fuel intensive case, which assumes a future world with extensive reliance on fossil fuels. Compared to preindustrial conditions, current era inorganic nitrogen inputs over the study period of 64 years modestly increased primary production, sinking particulate organic carbon (POC) export, and net ocean uptake from air-sea CO_2 flux. Increased atmospheric N inputs to otherwise N-limited regions stimulated primary production by small phytoplankton and diatoms, resulting in a reduction in N_2 fixation because diazotrophs were not able to compete as effectively for surface-dissolved P and Fe. The study suggested that new nitrogen inputs to the oceans via anthropogenic atmospheric N inputs could be partially compensated for by decreased N_2 fixation.

[12] In this paper we present results of transient sensitivity studies with the Biogeochemical Elemental Cycling (BEC) ocean model to increasing anthropogenic inorganic nitrogen and soluble iron from atmospheric processing of dust and combustion sources. After an initial preindustrial spin-up of 500 years, three sets of deposition data were employed as external forcings, linearly increasing over 150 years to capture the transition from the preindustrial era to current conditions. The deposition data sets included (1) variable mineral aerosol iron solubility combined with soluble iron from combustion sources; (2) increasing atmospheric inorganic nitrogen inputs; and (3) simultaneously increasing iron and nitrogen inputs. Global integrals and spatial patterns were calculated for each case for denitrification, N_2 fixation, primary production, sinking POC export at 103 m, excess inorganic nitrogen ($[NO_3^-] + [NH_4^+] - 16[PO_4^{3-}]$), sea-air CO_2 flux and atmospheric pCO_2. A key goal was to examine how increasing nitrogen and soluble iron inputs since the preindustrial era may be perturbing marine biogeochemical cycles.

2. Methods

[13] The BEC model simulations were carried out within the National Center for Atmospheric Research's (NCAR) Community Climate System Model 3 (CCSM) Parallel Ocean Program ocean module [*Collins et al.*, 2006; *Yeager et al.*, 2006]. The horizontal resolution of the model is variable such that globally it is on average 3.6° longitude/2.0° latitude but increases to approximately 3.6° longitude/0.9° latitude at the equator. In order to allow for computations of surface ocean pCO_2 and air-sea CO_2 flux, the ecosystem component of the BEC model [*Doney et al.*, 2009] is coupled to a carbonate chemistry module based on the Ocean Carbon Model Intercomparison Project (OCMIP) [*Doney et al.*, 2003, 2004, 2006].

[14] The marine ecosystem in the BEC model includes multiple, potentially growth-limiting nutrients (nitrogen, phosphorus, iron, and silicon). The growth of four phytoplankton functional groups, namely, picoplankton, diatoms, diazotrophs, and coccolithophores, were simulated along with the biogeochemical cycling of carbon, nitrogen, phosphorus, silicon, oxygen, alkalinity, and iron. Diazotrophs have higher iron and light requirements, higher N/P ratios, and slower maximum growth rates than the other phytoplankton groups. Detailed description of the model is available in the works of *Moore et al.* [2001, 2004]. Some parameter modifications [*Moore et al.*, 2006; *Krishnamurthy et al.*, 2007b] and additional improvements to the model are described by *Moore and Braucher* [2008].

[15] Relevant to this study, iron sources from mineral dust and sedimentary sources were included in the model [*Moore et al.*, 2001, 2004; *Moore and Braucher*, 2008]. The sedimentary iron source was weighted by the actual ocean bathymetry from ETOP2 version 2.0 2-min global gridded database [*U.S. Department of Commerce*, 2006]. Hence, at each cell in the model, the fraction of the cell area that would consist of sediments based on the high-resolution ETOP2V2 database was calculated. This provided a more realistic distribution of sedimentary iron sources and improved the match to observed iron distributions [*Moore and Braucher*, 2008]. The BEC model utilized a seawater iron scavenging parameterization based on simulated soluble iron concentration and number of particles available to scavenge iron; the effects of organic ligands are treated implicitly through nonlinearity in the scavenging rates, which increase at high iron concentrations [*Moore et al.*, 2004; *Moore and Braucher*, 2008].

[16] Dust deposition was from the climatology of *Luo et al.* [2003]. Atmospheric dust was assumed to contain a constant 30.8% Si and 0.105% P by weight; 7.5% of this Si and 15% of this P were treated as soluble [*Duce et al.*, 1991] and thus entered the dissolved silicate and phosphate pool upon deposition. Atmospheric inputs of inorganic nitrogen to oceans for the current era were obtained from University

of California Irvine Chemical Transport Model (UCICTM) simulations with an embedded inorganic aerosol thermodynamic equilibrium model [*Luo et al.*, 2007]. Preindustrial deposition estimates were obtained by removing anthropogenic sources from simulations with present-day meteorology. Details on the nitrogen input data sets are given by *Luo et al.* [2007] and *Krishnamurthy et al.* [2007a]. Variable solubility iron inputs were obtained from simulations by *Luo et al.* [2008]. Their study simulated the emission, transport, and deposition of soluble iron to surface oceans from combustion sources. Soluble iron estimates were obtained by employing a combination of cloud processing (acidity of cloud droplets converts insoluble Fe into soluble Fe) [*Hand et al.*, 2004; *Luo et al.*, 2005, 2008] and hematite chemical reactions (hematite in dust is a source of soluble iron) [*Meskhidze et al.*, 2003] on modeled combustion and dust distributions.

[17] Four sets of BEC ocean model simulations were performed. A 650-year control simulation was conducted with preindustrial variable solubility iron inputs from dust and combustion sources (only biomass burning under preindustrial). After model year 500, three 150-year transient branch simulations were conducted to model the temporal evolution from preindustrial to modern conditions; anthropogenic perturbations in iron and/or nitrogen deposition (modern minus preindustrial), increasing linearly with time, are added to the preindustrial control. The first set of simulations employed linearly increasing perturbations in variable aerosol iron solubility inputs from dust and combustion sources (Scenario III from *Luo et al.* [2008], but with a 50% reduction (from 4% to 2%) in combustion Fe initial solubility, as preliminary simulations suggested excessive iron inputs to the North Pacific with the original values), hereafter referred to as case 1. The spatial patterns of the anthropogenic perturbation (modern minus preindustrial) differ from preindustrial fields, and thus the transient experiments were not just a linear increase of preindustrial fields.

[18] The cloud processing under preindustrial era was similar to that under modern era, but the hematite processing was lowered because of lower levels of atmospheric sulfur dioxide. The cloud processing case as implemented in our model [*Hand et al.*, 2004; *Luo et al.*, 2005, 2008] assumes that the clouds are always sufficiently acidic to process the iron to become more soluble. Hence, solubility of iron depends only on whether the iron is in a cloud or not. No pH parameterizations are set in the cloud processing method. Under hematite processing [*Meskhidze et al.*, 2003], the acidity of the aerosol is critical for the conversion of Fe^{3+} to Fe^{2+}, and there anthropogenic sulfate does play an important role in modulating acidity. Here the pH values are set depending on the SO_4 concentration. Hence, we assumed that only the hematite processing case changes under the preindustrial conditions because of lower SO_4 levels. The preindustrial case did not include biofuel emissions of iron and assumed that biomass burning was reduced by 90% from contemporary levels.

[19] The second set (case 2) of simulations employed linearly increasing, anthropogenic atmospheric inorganic nitrogen inputs (obtained from simulations by *Luo et al.* [2007]). The third set (case 3) of simulations combined the above two cases to include linearly increasing anthropogenic iron and nitrogen inputs. Total simulated inorganic N deposition to the ocean was ~22 Tg N/a for the preindustrial and ~39 Tg N/a for the current era [*Krishnamurthy et al.*, 2007a]. Our preindustrial estimate is on the high end of recent estimates (~14 Tg N/a in the work of *Duce et al.* [2008]). The response to rising N inputs to the oceans in the current era may be underestimated compared to the ~47 Tg N/a in the work of *Duce et al.* [2008]. Total simulated soluble iron inputs to the global oceans were 2.4×10^9 mol Fe/a for the preindustrial and 5.5×10^9 mol Fe/a in the current era. Further details on atmospheric processing and combustion sources can be found in the work of *Luo et al.* [2008].

[20] Our approximation of a linear increase in soluble iron inputs was based in part on a recent study by *Bond et al.* [2007]. They found that black carbon emissions since the preindustrial era have increased almost linearly [*Bond et al.*, 2007, Figure 6]. In an earlier work, *Bond et al.* [2004] studied the role of combustion practices in the determination of emissions and found that 38%, 20%, and 42% of the black carbon emissions were from fossil fuel, biofuel, and open burning, respectively. Observations at Cheju, Korea, suggest a high correlation between soluble iron and black carbon coming from combustion sources [*Chuang et al.*, 2005]. Therefore, we used the linear increase in deposition of soluble iron from the preindustrial to modern values. In reality, increases in recent decades may have been somewhat more rapid than this linear trend. Also, this regional relation between soluble Fe and black carbon may vary, particularly with changes in the black carbon sources.

[21] In the preindustrial climate, mineral aerosol availability may have been different from present era conditions because of alterations in climate, hydrological cycle, and land use. For example, the intensity of cultivation in deserts would have been lower than that in modern era. Vegetation cover may also have differed because of climate and soil moisture trends and carbon dioxide fertilization effects from rising atmospheric pCO_2. We neglect for this study possible changes in mineral aerosols due to climate or land use between modern and preindustrial conditions, which could be large and perhaps dominate the anthropogenic signal, but remain largely uncertain even in terms of the sign of the anthropogenic trend [e.g., *Mahowald and Luo*, 2003; *Tegen et al.*, 2004; *Mahowald and Dufresne*, 2004; *Mahowald et al.*, 2009].

[22] A similar linear increase in anthropogenic atmospheric inorganic N inputs was assumed, but again, increases in recent decades in N inputs were likely more rapid. Atmospheric CO_2 concentration was modeled as a single, well-mixed box in contact with the oceans. Climate forcings and winds were from late 20th century NCAR-NCEP climatology [*Large and Yeager*, 2004].

[23] Ocean iron scavenging parameters were optimized with the modern era, variable solubility atmospheric iron inputs to provide the best match to observed iron distributions [following *Moore and Braucher*, 2008]. The higher soluble iron inputs in the variable aerosol iron solubility case, particularly in the North Pacific, required a higher base scavenging rate to keep simulated dissolved iron concentrations reasonable, compared with the fixed 2% solubility

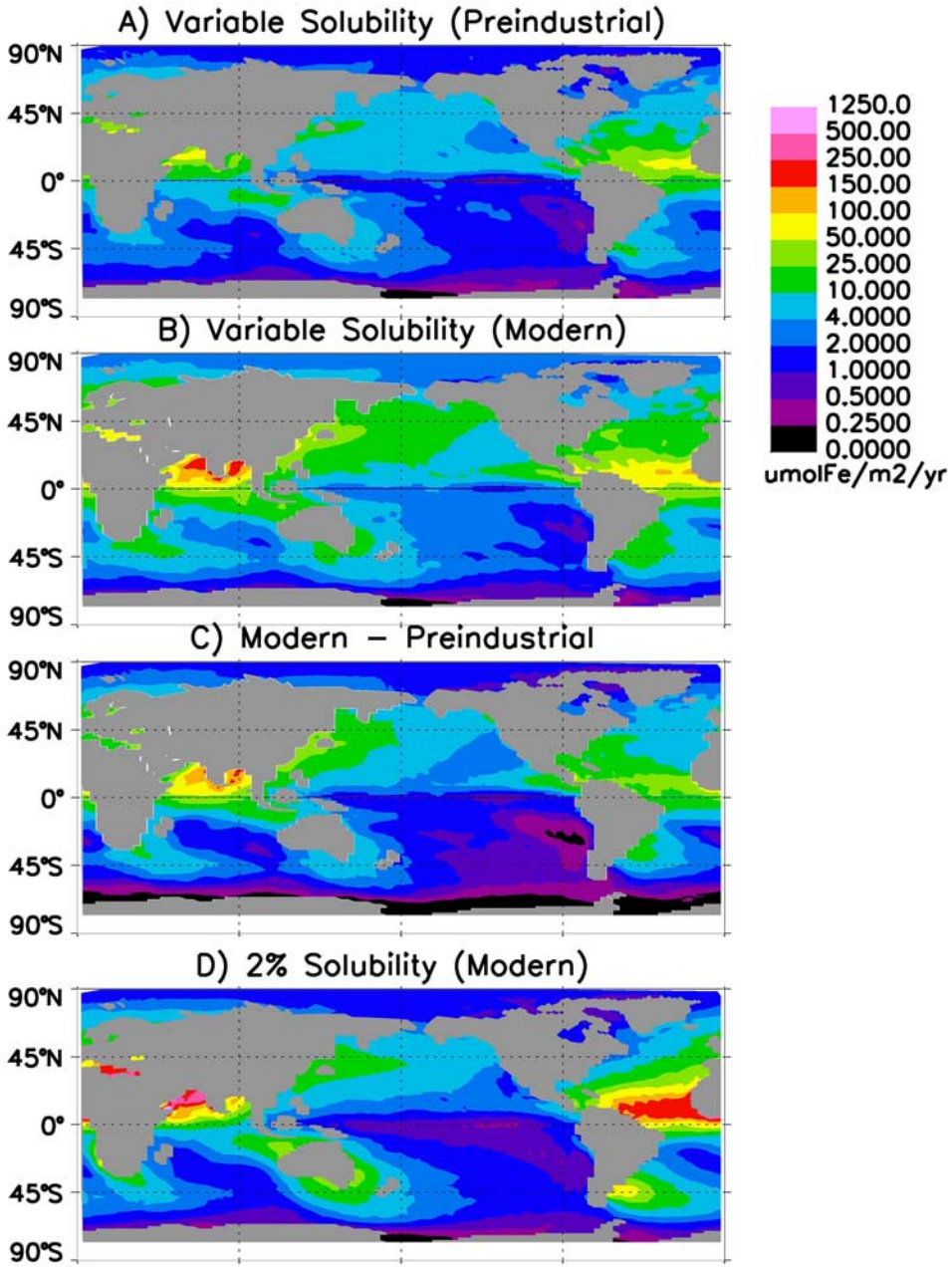

Figure 1. Spatial distributions of annual iron deposition under (a) preindustrial and (b) modern variable aerosol iron solubility and (c) their difference. (d) Annual iron deposition under globally constant (2%) aerosol iron solubility during the modern era.

used by *Moore and Braucher* [2008]. Conversely, lower iron inputs beneath the main dust plumes required a reduction in the scavenging coefficient that influenced scavenging at high iron concentrations (>0.6 nM) to best match observations. These optimized scavenging parameter values were utilized in all simulations.

3. Results

[24] Globally, we estimated that surface ocean soluble iron inputs to the contemporary ocean were more than double those during preindustrial times. The largest changes were in the northern Indian Ocean, the North Pacific, and the tropical North Atlantic (Figure 1c). Modest increases in soluble iron deposition were also observed in other remote regions compared to preindustrial. The influence of atmospheric processing in the presence of increased anthropogenic pollutants was particularly critical in remote regions away from major dust plumes (Figures 1b and 1d in the tropical and subtropical Pacific). Combustion sources of soluble iron were important near industrial and biomass burning sources where dust sources were lower (for exam-

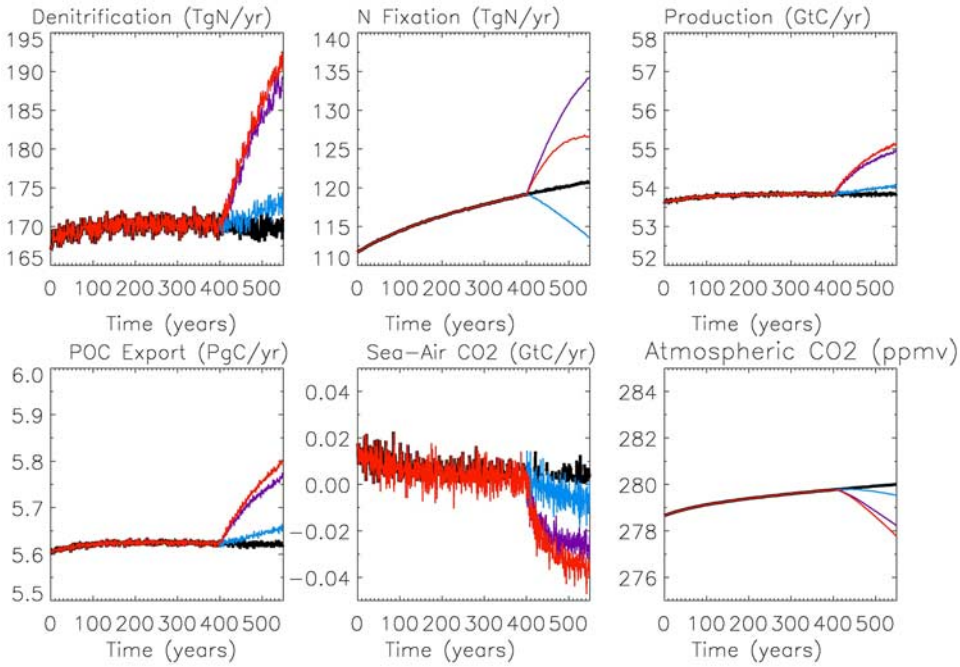

Figure 2. Changes in key biogeochemical fluxes over time for 550-year simulations; the first 100 years have been excluded in the plots for clarity; hence years 101 to 650 are shown. First 400 years depicts model spin-up. Last 150 years denote the transient experiment. Black line describes the preindustrial control, and cases 1 (Fe), 2 (N), and 3 (Fe+N) are depicted by violet, blue, and red lines, respectively.

ple, off the coast of South and East Asia). Solubilities less than 2% reduced iron inputs beneath the major dust plumes (i.e., tropical Atlantic, Figures 1b and 1d). In spite of combustion iron estimated as being the source of only 5% of total global iron inputs from the atmosphere to oceans, soluble iron inputs to surface oceans from combustion sources may exceed 50% in some regions [*Luo et al.*, 2008].

[25] Since the preindustrial era, anthropogenic inorganic nitrogen inputs to the ocean increased considerably, especially in coastal waters as well as in open ocean areas downwind of fossil-fuel-based industries and regions where intensive agriculture has resulted in increased fertilizer use [*Krishnamurthy et al.*, 2007a]. Nitrogen deposition increased significantly downwind of the coast of East and South Asia. An increase of >10 Tg N/a since preindustrial was seen off the east coast of North America and Europe. There was also a sizable increase in nitrogen deposition close to the African, Australian, and the South American continents. Compared to the preindustrial era, all the ocean basins except the Southern Ocean and the South Pacific Ocean had a substantial increase in nitrogen deposition [*Krishnamurthy et al.*, 2007a].

[26] Changes in key marine biogeochemical fluxes during the transient 150-year preindustrial to modern simulations suggest significant differences in oceanic biogeochemical cycling between the control and the three different atmospheric nutrient input regimes (Figure 2). Denitrification increased by ~20 Tg N/a in case 1 (Fe) and case 3 (Fe+N) under increasing anthropogenic soluble iron inputs compared to the preindustrial control, with a smaller ~5 Tg N/a increase in case 2 (N). Increasing iron (and nitrogen) inputs fueled additional export production above the oxygen minimum zones. The largest increase in nitrogen fixation was about ~15 Tg N/a in case 1 (Fe) followed by ~5 Tg N/a for case 3 (Fe+N) as increased soluble iron inputs relative to the control reduced the Fe limitation in diazotrophs (N fixers). Increased diazotroph Fe and P limitation reduced nitrogen fixation by ~5 Tg N/a in case 2 (N) as the diazotrophs were outcompeted by the diatoms and small phytoplankton under increased anthropogenic nitrogen inputs.

[27] Primary production increased from ~53.5 Pg C/a in preindustrial control to ~55 Pg C/a under case 3 (Fe+N), closely followed by case 1 (Fe). Case 2 (N) had only a marginal increase of ~0.5 Pg C/a in primary production compared to the preindustrial control. Case 3 (Fe+N) had the highest sinking particulate organic carbon (POC) flux at 103 m of ~5.8 Pg C/a closely followed by case 1 (Fe) with ~5.75 Pg C/a, whereas it was ~5.6 Pg C/a under preindustrial control. Sinking POC export increased only marginally (~0.05 Pg C/a) under case 2 (N) compared to the preindustrial control. Atmospheric CO_2 declined relative to control by ~1.8 ppm, ~0.5 ppm, and ~2.2 ppm at the end of the simulations for cases 1 (Fe), 2 (N), and 3 (Fe+N), respectively.

[28] Nitrogen fixation was higher in both the subtropical North and South Pacific and the South Atlantic in case 1 (Fe) compared to preindustrial control. Increased atmospheric processing resulted in higher modern soluble Fe inputs to these regions, which were away from major dust sources, partially relieving Fe limitation of diazotrophs (Figure 3b). There was a decrease in N_2 fixation in the

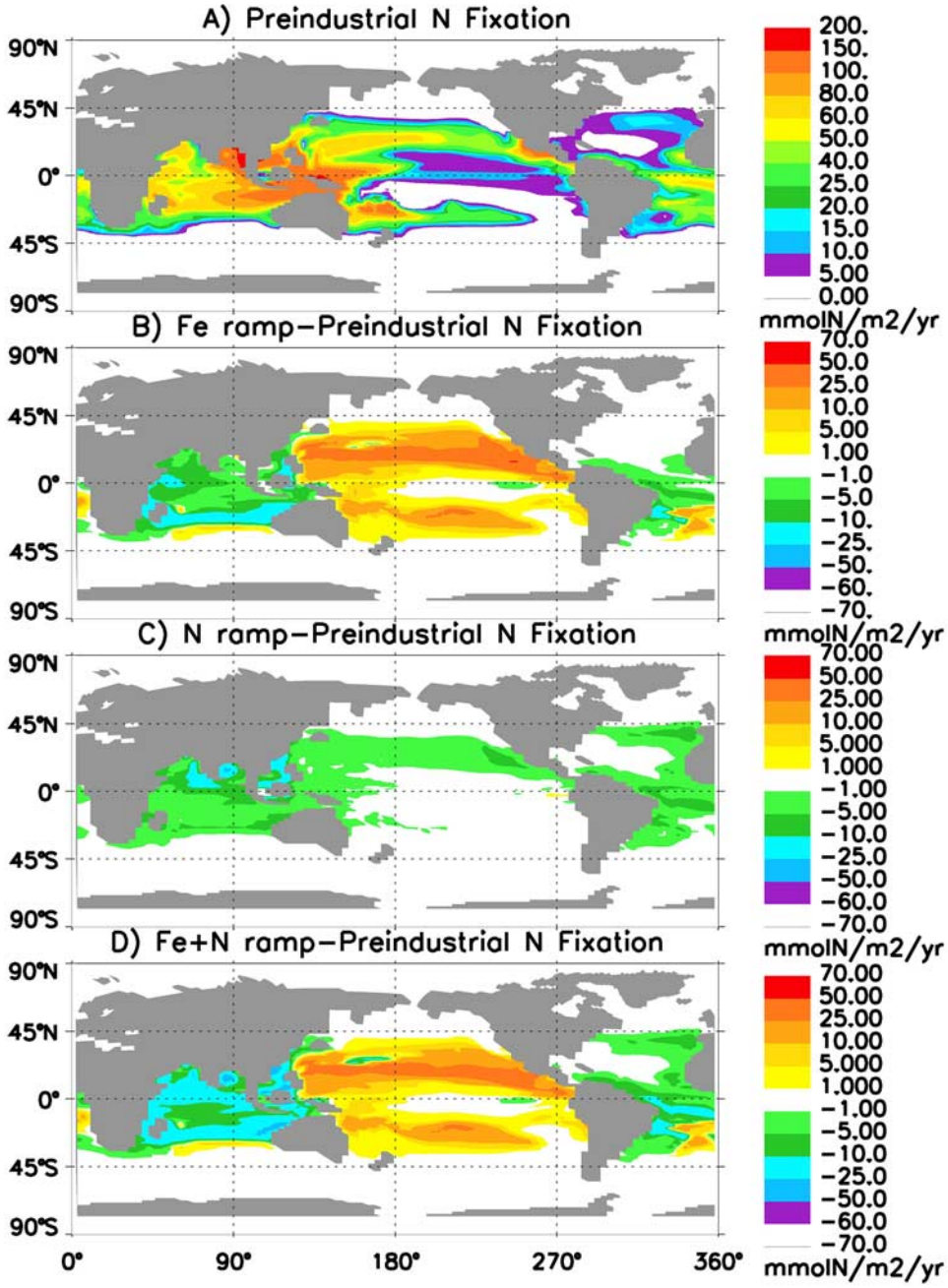

Figure 3. Global values of N fixation for the final year of simulations under (a) preindustrial with the difference between cases (b) 1 (Fe), (c) 2 (N), and (d) 3 (Fe+N) and preindustrial.

north Indian Ocean and equatorial Atlantic due to increased P limitation of diazotrophs, as less excess P was exported from the Pacific to the Indian Ocean and from the South Atlantic to the tropical Atlantic. Compared to preindustrial N_2 fixation decreased over the subtropical North Pacific, the Indian, and the Atlantic Ocean in case 2 (N) (Figure 3c). N_2 fixation increased in case 3 (Fe+N) compared to preindustrial because of increased soluble iron inputs in the subtropical North Pacific (Figure 3d). Increased Fe and P limitation of N fixers due to enhanced uptake by diatoms and small phytoplankton under higher N availability, however, resulted in a larger decrease in N_2 fixation in the Arabian Sea, Bay of Bengal, and across the Atlantic Ocean. Compared to the preindustrial control, simulated global N_2 fixation increased by ~11% and ~5% under cases 1 (Fe) and 3 (Fe+N), whereas it decreased by ~6% under case 2 (N).

[29] Atmospheric N deposition was ~2.4% and ~4.2% of sinking particulate organic nitrogen (PON) export for the preindustrial and the 1990s, respectively [*Krishnamurthy et al.*, 2007a]. In the same study, atmospheric N supported ~18% of sinking PON export in the western subtropical

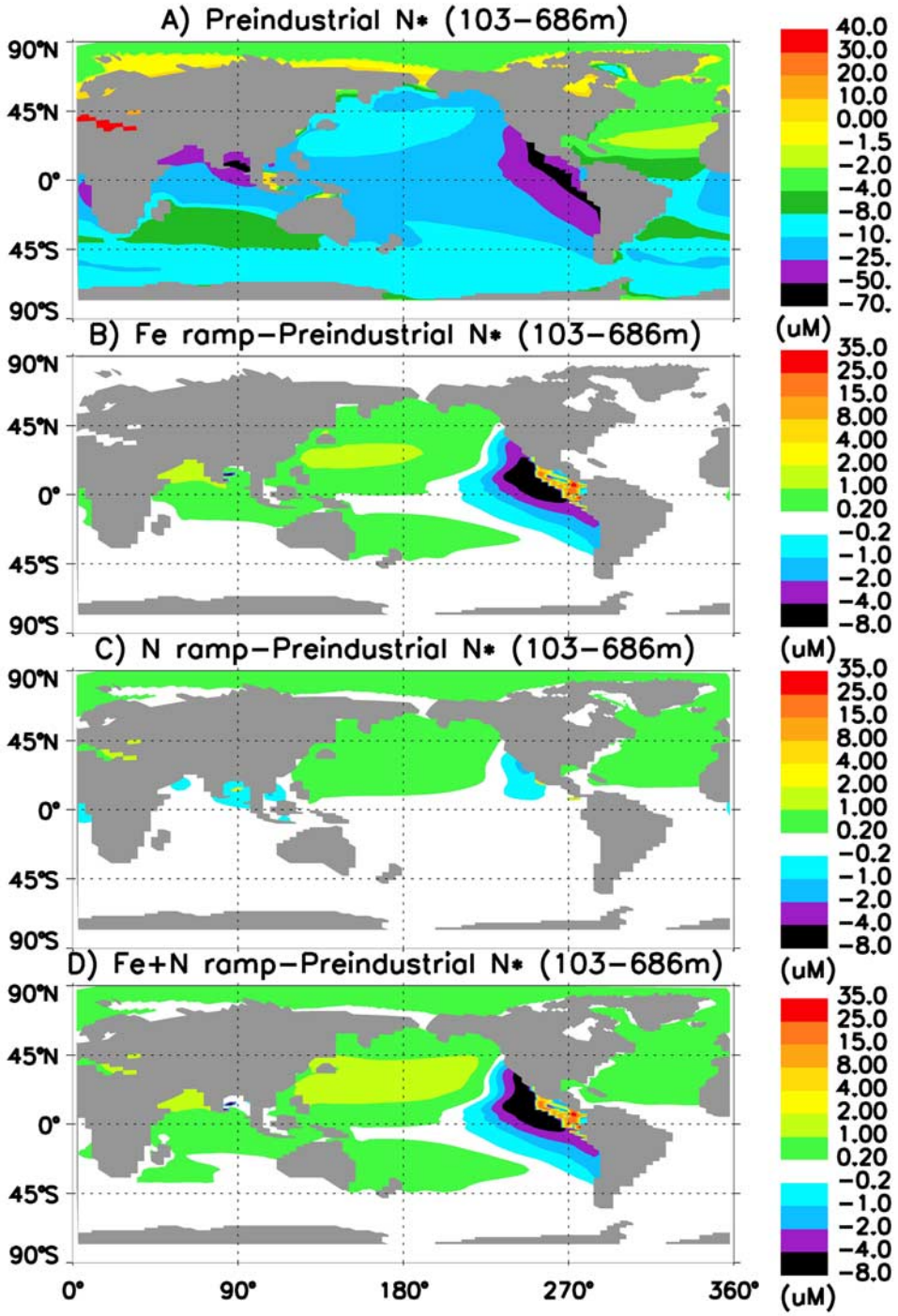

Figure 4. Global values of N averaged over the depths of 103 m to 686 m for the final year of simulations under (a) preindustrial with the difference between cases (b) 1 (Fe), (c) 2 (N), and (d) 3 (Fe+N) and preindustrial.

Pacific, ~6% in the Arabian Sea, and ~9% in the Bay of Bengal. For comparison, *Duce et al.* [2008] include both organic and inorganic nitrogen deposition over global oceans and estimated that ~3% of the annual new production could be accounted for by atmospheric deposition of anthropogenic nitrogen.

[30] A number of authors since Redfield have suggested using excess inorganic nitrogen relative to inorganic phosphorus at Redfield stoichiometry as a quasi-conservative tracer that reflects the net impact of N_2 fixation, denitrification, and other processes that add or remove fixed N but not P [e.g., *Michaels et al.*, 1996; *Gruber and Sarmiento*, 1997; *Gruber*, 2004]. Atmospheric deposition of Fe and N

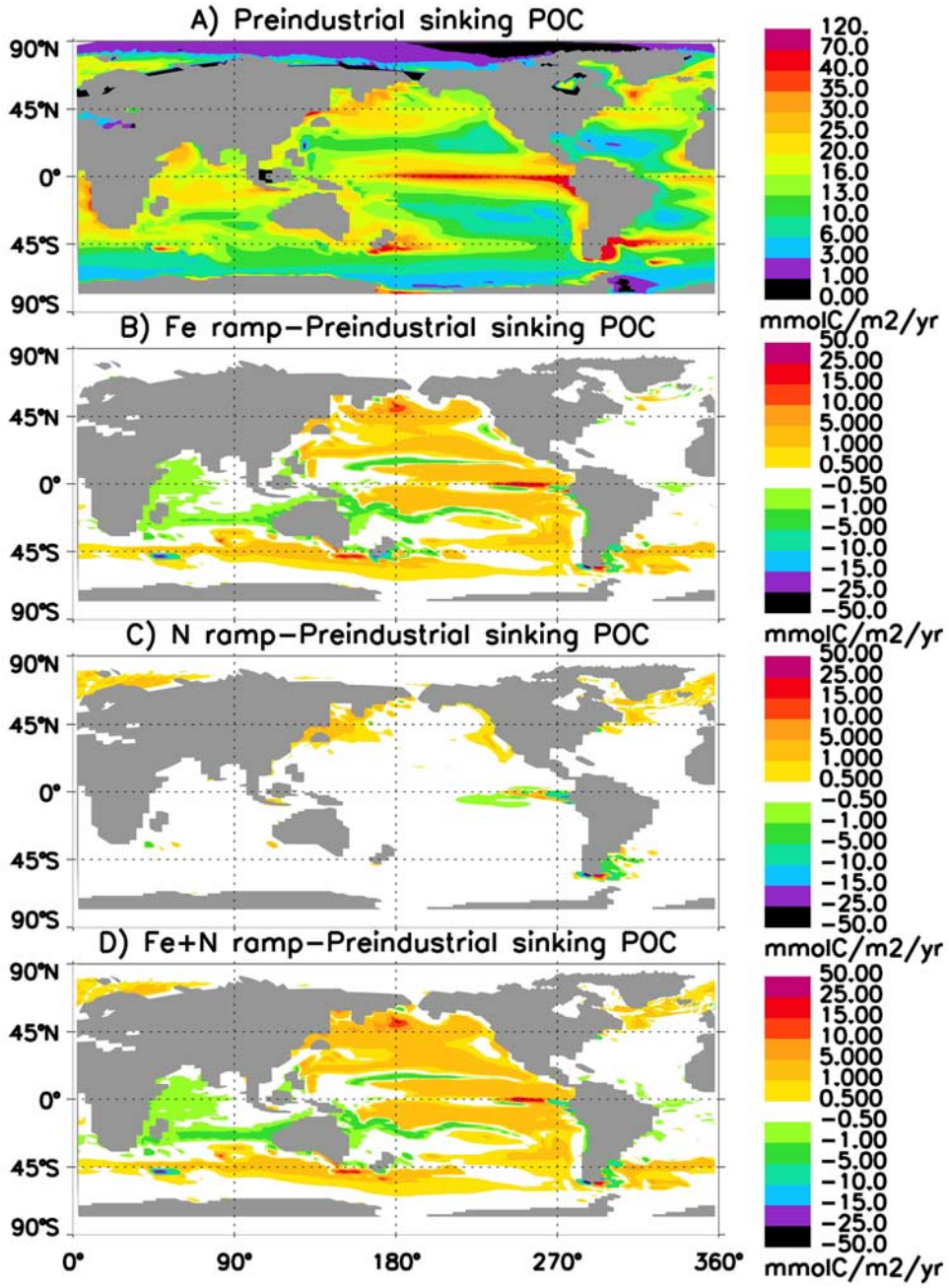

Figure 5. Global values of sinking particulate organic carbon (POC) export at 103 m for the final year of simulations under (a) preindustrial with the difference between cases (b) 1 (Fe), (c) 2 (N), and (d) 3 (Fe+N) and preindustrial.

can act to increase upper ocean excess inorganic nitrogen as Fe stimulates N_2 fixation and because the N/P ratios of N fixers are much higher than Redfield stochiometries [*Letelier and Karl*, 1996]; conversely, Fe inputs can lower excess inorganic nitrogen if the resulting elevated export production stimulates more denitrification.

[31] We examined the depth-averaged excess inorganic nitrogen ($[NO_3^-] + [NH_4^+] - 16[PO_4^{3-}]$) over the model upper thermocline (103 m to 686 m) (Figure 4). Compared to the preindustrial control (Figure 5a), cases 1 (Fe) and 3 (Fe+N) had increased nitrogen fixation under higher soluble iron inputs resulting in higher excess inorganic nitrogen values in the subtropical North Pacific. In the Arabian Sea, for cases 1 (Fe) and 3 (Fe+N), excess inorganic nitrogen increased despite lower values of N_2 fixation (Figure 3), in part because of low denitrification in our model in the oxygen minimum zones in this region [*Moore and Doney*, 2007]. Increased N_2 fixation under reduced Fe limitation resulted in increased excess inorganic nitrogen values right off the coast in the eastern equatorial Pacific (Figures 4b and 4d).

Table 1. Total Global Primary Production, N Fixation, Sinking POC From the Final Year of Simulation (Year 650), Atmospheric pCO_2 at the End of the 650 Year Simulations, Diatom, Small Phytoplankton, and Diazotroph Nutrient, and Light Limitation Factors over Global Ocean Area[a]

	Preindustrial	Case 1	Case 2	Case 3
Total primary production (Pg C/a)	53.65	54.75(+1.10)	53.84(+0.19)	54.95(+1.3)
Total nitrogen fixation (Tg N/a)	120.32	133.73(+13.41)	113.07(−7.25)	126.18(+5.86)
Total sinking POC (Pg C/a)	5.62	5.76(0.14)	5.65(0.03)	5.8(+0.18)
Final atmospheric PCO_2 (ppm/a)	280.005	278.237(−1.77)	279.531(−0.47)	277.784(−2.22)
Diatoms				
Fe-limited	34.11	28.95(−5.16)	34.74(+0.63)	29.08(−5.03)
N-limited	46.65	50.05(+3.4)	43.44(−3.21)	46.65(0)
P-limited	8.783	9.607(+0.82)	11.27(+2.48)	12.57(+3.79)
Si-limited	6.327	7.281(+0.95)	6.513(+0.19)	7.508(+1.18)
Light-limited	4.112	4.101(−0.011)	4.026(−0.09)	4.179(+0.07)
Small Phytoplankton				
Fe-limited	34.66	29.04(−5.62)	35.19(+0.53)	29.31(−5.35)
N-limited	43.99	48.15(+4.16)	41.37(−2.62)	45.28(+1.29)
P-limited	7.696	8.331(+0.64)	9.742(+2.046)	10.62(+2.92)
Light-limited	13.64	14.46(+0.82)	13.69(+0.05)	14.78(+1.14)
Diazotrophs				
Fe-limited	35.76	32.51(−3.25)	35.21(−0.55)	31.96(−3.8)
P-limited	26.74	29.8(+3.06)	27.37(+0.63)	30.47(+3.73)
Light-limited	2.332	2.525(+019)	2.25(−0.08)	2.401(+0.07)

[a]Values in parentheses are the difference of these values relative to the preindustrial control.

The increased export combined with the increased N_2 fixation resulted in increased denitrification in the eastern equatorial Pacific under cases 1 (Fe) and 3 (Fe+N), lower excess inorganic nitrogen compared to the preindustrial control further offshore. Under case 2 (N), compared to preindustrial control, increased nitrogen deposition resulted in higher excess inorganic nitrogen values throughout the North Atlantic and the North and South Pacific (Figure 4c).

[32] Changing atmospheric nutrient inputs modestly shifted spatial patterns of nutrient limitation. Compared to the preindustrial control, Fe-limited regions decreased by ∼5% in both cases 1 (Fe) and 3 (Fe+N) and increased by ∼1% under case 2 (N). N-limited regions increased by ∼5% under case 1 (Fe), decreased by ∼4% under case 2 (N), and remained the same under case 3 (Fe+N). P-limited regions increased by ∼1%, ∼3%, and ∼4% under cases 1 (Fe), 2 (N), and 3 (Fe+N), respectively. Si-limited regions increased by 2% to 4% under the three cases. Exact differences in nutrient-limited and light-limited areas between control and individual cases for small phytoplankton, diatoms, and diazotrophs are summarized in Table 1.

[33] We compare spatial maps from the end of the simulations to examine how increasing anthropogenic nitrogen and soluble iron inputs may be perturbing the global carbon cycle. The mean annual sinking POC export at 103 m increased in the North and South Pacific and the Southern Ocean compared with preindustrial conditions under cases 1 and 3 (Figures 5b and 5d), because of decreased iron limitation in the HNLC areas and increased N_2 fixation in the subtropics. This led to a net oceanic CO_2 uptake at the corresponding locations (Figures 6b and 6d). The upwelling of inorganic carbon-enriched waters as a result of increased export in the subtropics resulted in some increased CO_2 outgassing in the equatorial Pacific.

[34] There was a minimal change in sinking POC export under case 2 (N) in the North Atlantic, subarctic North Pacific, and the equatorial Pacific resulting in a small change in the sea-air CO_2 flux at the corresponding locations (Figures 5b and 6b). Sinking POC export at 103 m increased globally by 0.14 Pg C/a (or ∼2.5%), 0.03 Pg C/a (or ∼0.5%), and 0.18 Pg C/a (or ∼3.2%) since preindustrial under cases 1 (Fe), 2 (N), and 3 (Fe+N), respectively (Table 1).

[35] Overall, our simulations suggest that the influence of elevated human-induced soluble iron inputs alone as well as combined with increasing anthropogenic nitrogen inputs to global marine surface waters has a significant impact on marine biogeochemistry, particularly the nitrogen cycle and excess inorganic nitrogen distributions. Including only the increasing soluble iron, however, had a greater effect than anthropogenic nitrogen inputs alone on the sinking POC export and the air-sea CO_2 flux.

4. Discussion and Summary

[36] Recent studies suggest that regional variations in atmospheric iron inputs may have a significant impact on the spatial patterns and rates of marine nitrogen cycling. *Falcon et al.* [2004] measured in situ rates of N_2 fixation in the tropical North Atlantic (summer 2001 and spring 2002) and the subtropical North Pacific (fall 2002) near station ALOHA off Hawaii. They found that the higher aeolian iron inputs to the North Atlantic resulted in higher N_2 fixation rates, when compared to that at the site near station ALOHA. On the basis of cruise observations collected in the North Atlantic, North Pacific, western South Pacific, and the western North Atlantic, *Hynes et al.* [2009] found that *Trichodesmium* N_2 fixation rates were significantly higher in the subtropical North Atlantic than in the tropical and subtropical North and South Pacific. Their study suggested that *Trichodesmium* may be more P-limited in the North Atlantic, while they inferred that *Trichodesmium*

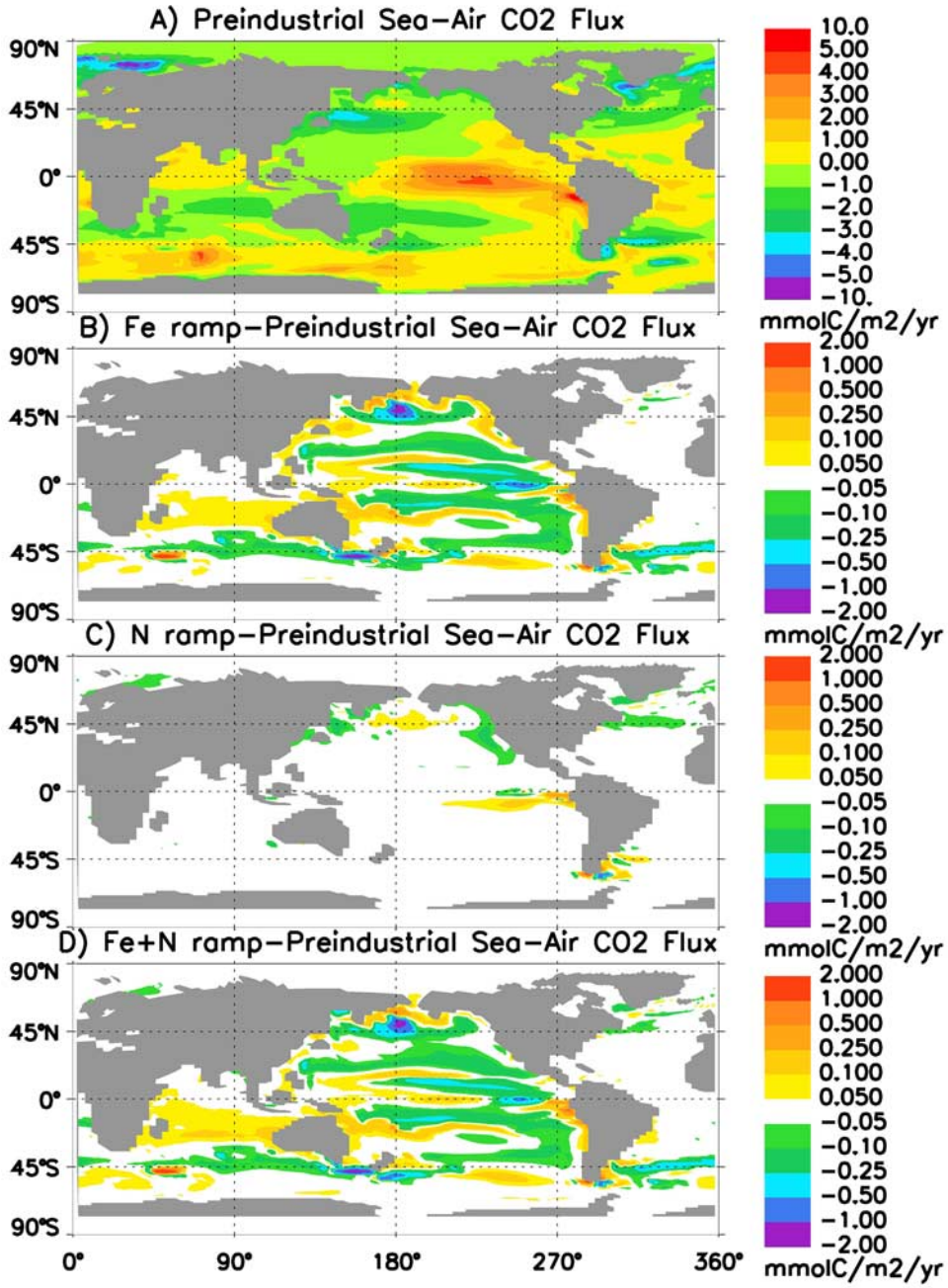

Figure 6. Global values of sea-air CO_2 flux for the final year of simulations under (a) preindustrial with the difference between cases (b) 1 (Fe), (c) 2 (N), and (d) 3 (Fe+N) and preindustrial.

may be more iron-limited in the North Pacific. *Moore et al.* [2006] suggested that N_2 fixation should be sensitive to iron inputs, particularly in the Pacific. There is increasing evidence for the importance of marine nitrogen fixers beyond *Trichodesmium* including unicellular and symbiotic cyanobacteria [*Church et al.*, 2008], though there is insufficient data on basin to global scale to fully characterize the nitrogen fixation rates of these other groups. *Deutsch et al.* [2007] argued that the North Pacific has higher N_2 fixation rates because of high water column denitrification, despite lower rates of atmospheric iron input.

[37] In the present paper, varying soluble aerosol iron deposition influenced the regional patterns of the simulated nitrogen cycle. Annual mean N_2 fixation increased substantially in some regions under increasing anthropogenic soluble iron inputs, especially across the North and South Pacific, with smaller changes in the Indian and Atlantic Ocean basins (Figure 3b). In the modern era, regions away from aeolian dust sources, like station ALOHA, receive substantially higher soluble iron inputs, in a fractional sense, relative to the preindustrial period. In this study, we model the atmospheric changes on aerosol iron solubility

since preindustrial explicitly; in contrast, the model ocean iron scavenging parameters are fixed in time and space across the control and transient simulations, and time varying changes in iron scavenging are included implicitly only through changes in particle load and soluble iron concentrations. It has been suggested by *Baker and Croot* [2009, and references therein] that oceanic controls, namely, seawater pH, presence of strong iron-binding ligands, iron associated with nanoparticle clusters, and organic colloids may play an important role in enhancing the solubility and bioavailability of aerosol-derived iron. They state that post-deposition processing of deposited aerosols, scavenging of dissolved iron by particles, and speciation could be key factors in the bioavailability of iron. Other than scavenging, these processes are largely neglected here.

[38] Estimates of N_2 fixation at station ALOHA (22.75°N, 158°W) from previous studies range between 31 and 51 mmol N/m^2/a [*Karl et al.*, 1997] to 30 and 282 mmol N/m^2/a [*Montoya et al.*, 2004]. N_2 fixation values for this region from our simulations were 55 mmol N/m^2/a, 80 mmol N/m^2/a, 53 mmol N/m^2/a, and 78 mmol N/m^2/a for the final year under preindustrial, case 1 (Fe), case 2 (N), and case 3 (Fe+N), respectively. At station ALOHA, the increase in N_2 fixation since preindustrial was 25 mmol N/m^2/a and 23 mmol N/m^2/a under cases 1 (Fe) and 3 (Fe+N), respectively.

[39] Using observational estimates of the sinking particulate organic nitrogen data at 150 m from station ALOHA, we calculated an increasing linear trend over 1989–2006 of 0.59 mmol N/m^2/a. Using the observational sinking particulate organic C flux at 150 m, and converting it to N with the Redfield ratio, we obtained an increasing trend of 0.23 mmol N/m^2/a. This value was similar to the iron-driven increase in N_2 fixation in our simulation (25 mmol N/m^2 in 150 years ~0.17 mmol N/m^2/a). Our model results likely underestimate the increases in iron solubility in recent decades, because of the assumed linear trend. Thus, our results suggest that increasing soluble iron inputs from the atmosphere may be contributing substantially to the shift toward increasing P limitation at station ALOHA. That is, a substantial part of the observed N_2 fixation increase may be due to the atmospheric deposition, rather than (or in addition to) decreases in mixed layer depth and changes in nutrient input from intermediate waters due to increased stratification as suggested previously [i.e., *Karl*, 1999].

[40] Hydrographic surveys have indicated that oceanic dissolved O_2 concentrations have changed, particularly during the later part of 20th century [*Keeling and Garcia*, 2002, and references therein]. *Manning and Keeling* [2006] estimated oceanic O_2 outgassing associated to global warming over 1993–2003 to be ~45 Tmol O_2/a. In our simulations, increasing soluble iron and nitrogen inputs increased oceanic O_2 outgassing by ~10 Tmol O_2/a in the modern era compared to the preindustrial control. Thus, biogeochemical trends may be significantly influencing air-sea O_2 flux, in addition to the temperature effects.

[41] Several studies have suggested a decreasing trend in the dissolved oxygen concentrations in the lower thermocline over the later part of the 20th century [*Joos et al.*, 2003] with the maximum observed change in the North Pacific [*Emerson et al.*, 2004]. The simulated subsurface dissolved O_2 distributions in the North Pacific in the present study were not significantly affected by the increases in export over the last few decades of the simulations. Our simulated changes to dissolved O_2 concentrations were much less than the trends in the observations for the North Pacific during 1980 to 2000 by *Emerson et al.* [2004] as well as those described in the simulations done by *Deutsch et al.* [2005, 2006]. This supports the idea that changes in physics (held constant in our simulations) and ventilation may be driving the observed changes in oxygen. The detection of long-term observational trends due to climate change and anthropogenic forcing are complicated by substantial interannual variability [*Mecking et al.*, 2008]. Recent modeling studies argue that the large trends in recent observational oxygen estimates may largely reflect natural climate variability rather than long-term secular trends [*Frölicher et al.*, 2009]. The significant changes in excess inorganic nitrogen distributions suggest that the excess inorganic nitrogen field is not static and may be a useful diagnostic of ongoing changes in ocean circulation and biogeochemistry that complements oxygen.

[42] Compared to the preindustrial era, increasing soluble iron inputs via combustion sources and atmospheric processing of mineral aerosols along with atmospheric anthropogenic nitrogen inputs resulted in a maximum global increase in primary production by ~2.4% in our simulations. This increased the sinking POC export at 103 m by ~3.2% leading to a reduction in atmospheric pCO_2 by ~2.2 ppm. This atmospheric CO_2 reduction is small compared with the observed increase of ~100 ppm, but would likely continue to increase in the coming decades as nutrient inputs to the oceans continue to rise (Figure 2). Extending our simulations with increasing iron and nitrogen inputs for another 100 years at the same linear rate resulted in ~4 ppm decrease in atmospheric pCO_2 compared to preindustrial control. The significant sedimentary iron source reduces the model sensitivity to variations in atmospheric iron inputs [*Moore and Braucher*, 2008].

[43] Several modeling studies have estimated changes in oceanic CO_2 uptake since preindustrial conditions by applying various scenarios of atmospheric CO_2 increase in the 21st century [*Sarmiento and Le Quéré*, 1996; *Sarmiento et al.*, 1998; *Joos et al.*, 1999; *Matear and Hirst*, 1999; *Greenblatt and Sarmiento*, 2004]. Compared to preindustrial conditions, these studies estimate that under the current era, there would be an increase in oceanic CO_2 uptake due to biology (by ~6–27%) but decreased oceanic CO_2 uptake due to changes in stratification (by ~3–20%) and CO_2 solubility (by ~9–14%) due to warming of surface waters [*Sabine and Feely*, 2007, and references therein]. Our results isolate the anthropogenic-nutrient-deposition-driven ocean biogeochemical response. This response is relatively modest at present (−2 ppm CO_2) but growing and could be important, especially when combined with the above mentioned climate-driven modifications and additional nutrient perturbations from riverine sources. Hence, these factors need to be considered when assessing the anthropogenic impacts on marine ecosystem productivity, air-sea CO_2 fluxes, and the global carbon cycle.

[44] The present work highlights the importance of studying the effects of varying iron solubility on oceanic ecosystems on a global scale. Better understanding of the mechanisms by which soluble iron is delivered to the surface ocean from anthropogenic environmental changes is required. This could be critical in providing improved estimates of bioavailable iron inputs to areas remote from aeolian dust sources. Modifications to iron solubility may occur in the near future based on what energy choices humans make. Enhanced fossil fuels usage and coal-based technology in the future would influence iron solubility closer to source regions as well as impact atmospheric anthropogenic N inputs. Better understanding of the availability of atmospheric organic nitrogen inputs and the bioavailability of the atmospheric N is needed [*Duce et al.*, 2008].

[45] Ongoing changes due to increased nitrate release from land due to fertilizer use as well as nitrogen deposition from the atmosphere in highly polluted areas [*De Leeuw et al.*, 2001], combined with a decrease of dust mobilization and transport in a warmer climate [*Werner et al.*, 2002; *Mahowald and Luo*, 2003], will impact atmospheric iron and nitrogen availability to surface oceans. Some studies also suggest that there could be an increase in dust loads due to changes in land use [*Tegen et al.*, 2004] and in vegetation cover [*Woodward et al.*, 2005]. Increasing pollution would affect atmospheric processing of mineral dust, in turn affecting aerosol iron solubility and hence, marine ecosystem bioavailability. On the other hand, a shift toward renewable energy sources for meeting greenhouse gas emission reduction goals would likely decrease iron solubility and nitrogen inputs into the atmosphere because of changes in combustion sources and atmospheric processes. Future simulations could include variable aerosol iron solubility derived from mineral dust and combustion sources under different emission, climate, and energy use scenarios to better understand the consequences of alternative energy strategies.

[46] **Acknowledgments.** This work was supported by funding from NSF grant OCE-0452972 to J. K. Moore and C. S. Zender. Computations were supported by the Earth System Modeling Facility at UCI (NSFATM-O321380) and by the Climate Simulation Laboratory at National Center for Atmospheric Research. The National Center for Atmospheric Research is sponsored by the U.S. National Science Foundation. N.M. would like to acknowledge the assistance of NSF–Carbon and Water (ATM-0628472), and N.M., S.D., and C.L. would like to acknowledge the assistance of NASA-IDS (NNX07AL80G).

References

Aguilar-Islas, A. M., J. Wu, R. Rember, A. M. Johansen, and L. M. Shank (2009), Dissolution of aerosol-derived iron in seawater: Leach solution chemistry, aerosol type, and colloidal iron fraction, *Mar. Chem.*, doi:10.1016/j.marchem.2009.01.011.

Aumont, O., E. Maier-Reimer, S. Blain, and P. Monfray (2003), An ecosystem model of the global ocean including Fe, Si, P co-limitations, *Global Biogeochem. Cycles*, *17*(2), 1060, doi:10.1029/2001GB001745.

Baker, A. R., and P. L. Croot (2009), Atmospheric and marine controls on aerosol iron solubility in seawater, *Mar. Chem.*, doi:10.1016/j.marchem.2008.09.003, in press.

Baker, A. R., T. D. Jickells, M. Witt, and K. L. Linge (2006), Trends in the solubility of iron, aluminium, manganese and phosphorus in aerosol collected over the Atlantic Ocean, *Mar. Chem.*, *98*(1), 43–58, doi:10.1016/j.marchem.2005.06.004.

Berman-Frank, I., J. T. Cullen, Y. Shaked, R. M. Sherrell, and P. G. Falkowski (2001), Iron availability, cellular iron quotas, and N fixation in Trichodesmium, *Limnol. Oceanogr.*, *46*, 1249–1260.

Bond, T. C., D. G. Streets, K. F. Yarber, S. M. Nelson, J.-H. Woo, and Z. Klimont (2004), A technology-based global inventory of black and organic carbon emissions from combustion, *J. Geophys. Res.*, *109*, D14203, doi:10.1029/2003JD003697.

Bond, T. C., E. Bhardwaj, R. Dong, R. Jogani, S. Jung, C. Roden, D. G. Streets, and N. M. Trautmann (2007), Historical emissions of black and organic carbon aerosol from energy-related combustion, 1850–2000, *Global Biogeochem. Cycles*, *21*, GB2018, doi:10.1029/2006GB002840.

Bouwman, A. F., L. J. M. Boumans, and N. H. Batjes (2002), Modeling global annual N_2O and NO emissions from fertilized fields, *Global Biogeochem. Cycles*, *16*(4), 1080, doi:10.1029/2001GB001812.

Boyd, P. W., and D. Mackie (2008), Comment on "The Southern Ocean biological response to aeolian iron deposition," *Science*, *319*, 159, doi:10.1126/science.1149884.

Boyd, P. W., et al. (2000), A mesoscale phytoplankton bloom in the polar Southern Ocean stimulated by iron fertilization, *Nature*, *407*(6805), 695–702, doi:10.1038/35037500.

Boyd, P. W., et al. (2004), The decline and fate of an iron-induced phytoplankton bloom, *Nature*, *428*, 549–553, doi:10.1038/nature02437.

Boyd, P. W., et al. (2007), Mesoscale iron enrichment experiments 1993–2005: Synthesis and future directions, *Science*, *315*, 612–617, doi:10.1126/science.1131669.

Cassar, N., M. L. Bender, B. A. Barnett, S. Fan, W. J. Moxim, H. Levy, and B. Tilbrook (2007), The Southern Ocean biological response to aeolian iron deposition, *Science*, *317*, 1067–1070, doi:10.1126/science.1144602.

Chen, Y., and R. L. Siefert (2004), Seasonal and spatial distributions and dry deposition fluxes of atmospheric total and labile iron over the tropical and subtropical North Atlantic Ocean, *J. Geophys. Res.*, *109*, D09305, doi:10.1029/2003JD003958.

Chuang, P., et al. (2005), The origin of water soluble particulate iron in the Asian atmospheric outflow, *Geophys. Res. Lett.*, *32*, L07813, doi:10.1029/2004GL021946.

Church, M. J., K. M. Bjorkman, D. M. Karl, M. A. Saito, and J. P. Zehr (2008), Regional distributions of nitrogen fixing bacteria in the Pacific Ocean, *Limnol. Oceanogr.*, *53*, 63–77.

Coale, K. H., et al. (1996), A massive phytoplankton bloom induced by an ecosystem-scale iron fertilization experiment in the equatorial Pacific Ocean, *Nature*, *383*, 495–501, doi:10.1038/383495a0.

Collins, W. D., et al. (2006), The Community Climate System Model version 3(CCSM3), *J. Clim.*, *19*(11), 2122–2143, doi:10.1175/JCLI3761.1.

de La Rocha, C. L. (2003), The biological pump, in *Treatise on Geochemistry*, vol. 6, edited by H. Elderfield, pp. 83–111, Elsevier, New York.

De Leeuw, G., et al. (2001), Atmospheric input of nitrogen into the North Sea: ANICE project overview, *Cont. Shelf Res.*, *21*(18–19), 2073–2094, doi:10.1016/S0278-4343(01)00043-7.

Desboeufs, K. V., R. Losno, and J. L. Colin (2001), Factors influencing aerosol solubility during cloud processes, *Atmos. Environ.*, *35*, 3529–3537, doi:10.1016/S1352-2310(00)00472-6.

Deutsch, C., S. Emerson, and L. Thompson (2005), Fingerprints of climate change in North Pacific oxygen, *Geophys. Res. Lett.*, *32*, L16604, doi:10.1029/2005GL023190.

Deutsch, C., S. Emerson, and L. Thompson (2006), Physical-biological interactions in North Pacific oxygen variability, *J. Geophys. Res.*, *111*, C09S90, doi:10.1029/2005JC003179.

Deutsch, C., J. L. Sarmiento, D. M. Sigman, N. Gruber, and J. P. Dunne (2007), Spatial coupling of nitrogen inputs and losses in the ocean, *Nature*, *445*(7124), 163–167, doi:10.1038/nature05392.

Doney, S. C., K. Lindsay, and J. K. Moore (2003), Global ocean carbon cycle modeling, in *Ocean Biogeochemistry: A JGOFS Synthesis*, edited by M. Fashom, pp. 217–238, Springer, New York.

Doney, S. C., et al. (2004), Evaluating global ocean carbon models: The importance of realistic physics, *Global Biogeochem. Cycles*, *18*, GB3017, doi:10.1029/2003GB002150.

Doney, S. C., K. Lindsay, I. Fung, and J. John (2006), Natural variability in a stable, 1000-yr global coupled climate-carbon cycle simulation, *J. Clim.*, *19*(13), 3033–3054, doi:10.1175/JCLI3783.1.

Doney, S. C., N. Mahowald, I. Lima, R. A. Feely, F. T. Mackenzie, and F. Lamarque (2007), The impacts of anthropogenic nitrogen and sulfur deposition on ocean acidification and the inorganic carbon system, *Proc. Natl. Acad. Sci. U. S. A.*, *104*, 14,580–14,585.

Doney, S. C., I. Lima, J. K. Moore, K. Lindsay, M. J. Behrenfeld, T. K. Westberry, N. Mahowald, D. M. Glover, and T. Takahashi (2009), Skill metrics for confronting global upper ocean ecosystem-biogeochemistry models against field and remote sensing data, *J. Mar. Syst.*, *76*, 95–112, doi:10.1016/j.jmarsys.2008.05.015.

Duce, R. A., et al. (1991), The atmospheric input of trace species to the world ocean, *Global Biogeochem. Cycles*, *5*, 193–259, doi:10.1029/91GB01778.

Duce, R., et al. (2008), Impacts of atmospheric anthropogenic nitrogen on the open ocean, *Science*, *320*, 893–897, doi:10.1126/science.1150369.

Emerson, S., Y. W. Watanabe, T. Ono, and S. Mecking (2004), Temporal trends in apparent oxygen utilization in the upper pycnocline of the North Pacific: 1980–2000, *J. Oceanogr.*, *60*, 139–147, doi:10.1023/B:JOCE.0000038323.62130.a0.

Falcon, L. I., E. J. Carpenter, F. Cipriano, B. Bergman, and D. G. Capone (2004), N_2 fixation by unicellular bacterioplankton from the Atlantic and Pacific Oceans: Phylogeny and in situ rates, *Appl. Environ. Microbiol.*, *70*, 765–770, doi:10.1128/AEM.70.2.765-770.2004.

Falkowski, P. G. (1997), Evolution of the nitrogen cycle and its influence on the biological sequestration of CO_2 in the ocean, *Nature*, *387*, 272–275, doi:10.1038/387272a0.

Falkowski, P. G., R. T. Barber, and V. Smetacek (1998), Biogeochemical controls and feedbacks on ocean primary production, *Science*, *281*, 200–206, doi:10.1126/science.281.5374.200.

Fan, S.-M., W. J. Moxim, and H. Levy II (2006), Aeolian input of bioavailable iron to the ocean, *Geophys. Res. Lett.*, *33*, L07602, doi:10.1029/2005GL024852.

Frölicher, T. L., F. Joos, G.-K. Plattner, M. Steinacher, and S. C. Doney (2009), Natural variability and anthropogenic trends in oceanic oxygen in a coupled carbon cycle-climate model ensemble, *Global Biogeochem. Cycles*, *23*, GB1003, doi:10.1029/2008GB003316.

Fung, I. Y., S. K. Meyn, I. Tegen, S. C. Doney, J. G. John, and J. K. B. Bishop (2000), Iron supply and demand in the upper ocean, *Global Biogeochem. Cycles*, *14*, 281–295, doi:10.1029/1999GB900059.

Galloway, J. N., et al. (2004), Nitrogen cycles: Past, present, and future, *Biogeochemistry*, *70*(2), 153–226, doi:10.1007/s10533-004-0370-0.

Greenblatt, J. B., and J. L. Sarmiento (2004), Variability and climate feedback mechanisms in ocean uptake of CO_2, in *The Global Carbon Cycle: Integrating Humans, Climate, and the Natural World*, edited by C. B. Field and M. R. Raupach, pp. 257–275, Island Press, Washington.

Gregg, W., P. Ginoux, P. S. Schopf, and N. W. Casey (2003), Phytoplankton and iron: Validation of a global three-dimensional ocean biogeochemical model, *Deep Sea Res., Part II*, *50*, 3143–3169, doi:10.1016/j.dsr2.2003.07.013.

Gruber, N. (2004), The dynamics of the marine nitrogen cycle and its influence on atmospheric CO_2 variations, in *The Ocean Carbon Cycle*, edited by M. Follows and T. Oguz, pp. 97–148, Springer, New York.

Gruber, N., and J. L. Sarmiento (1997), Global patterns of marine nitrogen fixation and denitrification, *Global Biogeochem. Cycles*, *11*, 235–266, doi:10.1029/97GB00077.

Guieu, C., S. Bonnet, T. Wagener, and M.-D. Loye-Pilot (2005), Biomass burning as a source of dissolved iron to the open ocean?, *Geophys. Res. Lett.*, *32*, L19608, doi:10.1029/2005GL022962.

Hand, J. L., N. Mahowald, Y. Chen, R. Siefert, C. Luo, A. Subramaniam, and I. Fung (2004), Estimates of soluble iron from observations and a global mineral aerosol model: Biogeochemical implications, *J. Geophys. Res.*, *109*, D17205, doi:10.1029/2004JD004574.

Holland, E. A., F. J. Dentener, B. H. Braswell, and J. M. Sulzman (1999), Contemporary and pre-industrial reactive nitrogen budgets, *Biogeochemistry*, *46*, 7–43.

Hynes, A. M., P. D. Chappell, S. T. Sonya, S. C. Doney, and E. A. Webb (2009), Cross-basin comparison of phosphorus stress and nitrogen fixation in *Trichodesmium*, *Limnol. Oceanogr.*, *54*(5), 1438–1448.

Intergovernmental Panel on Climate Change (2001), *Climate Change 2001: The Scientific Basis. Contribution of Working Group 1 to the Third Assessment Report of the Intergovernmental Panel on Climate Change*, Cambridge Univ. Press, Cambridge, U. K.

Jickells, T., and L. Spokes (2001), Atmospheric iron inputs to the oceans, in *Biogeochemistry of Iron in Seawater*, vol. 7, edited by D. R. Turner and K. Hunteger, pp. 85–121, John Wiley, Chichester, U. K.

Jickells, T., et al. (2005), Global iron connections between dust, ocean biogeochemistry and climate, *Science*, *308*, 67–71, doi:10.1126/science.1105959.

Johansen, A. M., R. L. Siefert, and M. R. Hoffman (2000), Chemical composition of aerosols collected over the tropical North Atlantic Ocean, *J. Geophys. Res.*, *105*, 15,277–15,312, doi:10.1029/2000JD900024.

Joos, F., G.-K. Plattner, T. F. Stocker, O. Marchal, and A. Schmittner (1999), Global warming and marine carbon cycle feedbacks on future atmospheric CO_2, *Science*, *284*, 464–467, doi:10.1126/science.284.5413.464.

Joos, F., G. K. Plattner, T. F. Stocker, A. Körtzinger, and D. W. R. Wallace (2003), Trends in marine dissolved oxygen: Implications for ocean circulation changes and the carbon budget, *Eos Trans. AGU*, *84*(21), 197–201, doi:10.1029/2003EO210001.

Karl, D. M. (1999), A sea of change: Biogeochemical variability in the North Pacific subtropical gyre, *Ecosystems*, *2*(3), 181–214.

Karl, D., R. Letelier, L. Tupas, J. Dore, J. Christian, and D. Hebel (1997), The role of N-fixation in biogeochemical cycling in the subtropical North Pacific Ocean, *Nature*, *388*, 533–538, doi:10.1038/41474.

Keeling, R. F., and H. E. Garcia (2002), The change in oceanic O_2 inventory associated with recent global warming, *Proc. Natl. Acad. Sci. U. S. A.*, *99*, 7848–7853, doi:10.1073/pnas.122154899.

Krishnamurthy, A., J. K. Moore, C. S. Zender, and C. Luo (2007a), Effects of atmospheric inorganic nitrogen deposition on ocean biogeochemistry, *J. Geophys. Res.*, *112*, G02019, doi:10.1029/2006JG000334.

Krishnamurthy, A., et al. (2007b), The effects of dilution and mixed layer depth on deliberate ocean iron fertilization: 1-D simulations of the southern ocean iron experiment (SOFeX), *J. Mar. Syst.*, *71*, 112–130, doi:10.1016/j.jmarsys.2007.07.002.

Lamarque, J.-F., et al. (2005a), Coupled chemistry-climate response to changes in aerosol emissions: Global impact on the hydrological cycle and the tropospheric burdens of OH, ozone and NOx, *Geophys. Res. Lett.*, *32*, L16809, doi:10.1029/2005GL023419.

Large, W. G., and S. G. Yeager (2004), Diurnal to decadal global forcing for ocean and sea-ice models: The data sets and flux climatologies, *NCAR Tech. Note, NCAR/TN-460*, 111, pp.

Letelier, R. M., and D. M. Karl (1996), Role of *Trichodesmium spp.* in the productivity of the subtropical North Pacific Ocean, *Mar. Ecol. Prog. Ser.*, *133*, 263–273, doi:10.3354/meps133263.

Luo, C., N. Mahowald, and J. del Corral (2003), Sensitivity study of meteorological parameters on mineral aerosol mobilization, transport and distribution, *J. Geophys. Res.*, *108*(D15), 4447, doi:10.1029/2003JD003483.

Luo, C., N. M. Mahowald, N. Meskhidze, Y. Chen, R. L. Siefert, A. R. Baker, and A. M. Johansen (2005), Estimation of iron solubility from observations and a global aerosol model, *J. Geophys. Res.*, *110*, D23307, doi:10.1029/2005JD006059.

Luo, C., C. S. Zender, H. Bian, and S. Metzger (2007), Role of ammonia chemistry and coarse mode aerosols in global climatological inorganic aerosol distributions, *Atmos. Environ.*, *41*, 2510–2533, doi:10.1016/j.atmosenv.2006.11.030.

Luo, C., N. Mahowald, T. Bond, P. Y. Chuang, P. Artaxo, R. Siefert, Y. Chen, and J. Schauer (2008), Combustion iron distribution and deposition, *Global Biogeochem. Cycles*, *22*, GB1012, doi:10.1029/2007GB002964.

Mahowald, N. M., and J.-L. Dufresne (2004), Sensitivity of TOMS aerosol index to boundary layer height: Implications for detection of mineral aerosol sources, *Geophys. Res. Lett.*, *31*, L03103, doi:10.1029/2003GL018865.

Mahowald, N. M., and C. Luo (2003), A less dusty future?, *Geophys. Res. Lett.*, *30*(17), 1903, doi:10.1029/2003GL017880.

Mahowald, N. M., A. R. Baker, G. Bergametti, N. Brooks, R. A. Duce, T. D. Jickells, N. Kubilay, J. M. Prospero, and I. Tegen (2005), Atmospheric global dust cycle and iron inputs to the ocean, *Global Biogeochem. Cycles*, *19*, GB4025, doi:10.1029/2004GB002402.

Mahowald, N. M., et al. (2009), Atmospheric Iron deposition: Global distribution, variability and human perturbations, *Annu. Rev. Mar. Sci.*, *1*, 245–278, doi:10.1146/annurev.marine.010908.163727.

Manning, A. C., and R. F. Keeling (2006), Global oceanic and land biotic carbon sinks from the Scripps atmospheric oxygen flask sampling network, *Tellus, Ser. B*, *58*, 95–116.

Martin, J. H. (1990), Glacial-interglacial CO_2 change: The iron hypothesis, *Paleoceanography*, *5*(1), 1–13, doi:10.1029/PA005i001p00001.

Matear, R. J., and A. C. Hirst (1999), Climate change feedback on the future oceanic CO_2 uptake, *Tellus, Ser. B*, *51*, 722–733.

Mecking, S., C. Langdon, R. A. Feely, C. L. Sabine, C. A. Deutsch, and D.-H. Min (2008), Climate variability in the North Pacific thermocline diagnosed from oxygen measurements: An update based on the U.S. CLIVAR/CO_2 Repeat Hydrography cruises, *Global Biogeochem. Cycles*, *22*, GB3015, doi:10.1029/2007GB003101.

Meskhidze, N., W. L. Chameides, A. Nenes, and G. Chen (2003), Iron mobilization in mineral dust: Can anthropogenic SO_2 emissions affect ocean productivity?, *Geophys. Res. Lett.*, *30*(21), 2085, doi:10.1029/2003GL018035.

Meskhidze, N., A. Nenes, W. Conant, and J. Seinfeld (2005), Evaluation of a new cloud droplet activation parameterization with in situ data from CRYSTAL-FACE and CSTRIPE, *J. Geophys. Res.*, *110*, D16202, doi:10.1029/2004JD005703.

Michaels, A. F., D. Olson, J. L. Sarmiento, J. W. Ammerman, K. Fanning, R. Jahnke, A. H. Knap, F. Lipschultz, and J. M. Prospero (1996), Inputs,

losses and transformations of nitrogen and phosphorus in the pelagic North Atlantic Ocean, *Biogeochemistry*, *35*, 181–226, doi:10.1007/BF02179827.

Michaels, A. F., D. M. Karl, and D. G. Capone (2001), Elemental stoichiometry, new production, and N fixation, *Oceanography*, *14*(4), 68–77.

Montoya, J., C. M. Holl, J. P. Zehr, A. Hansen, T. A. Villareal, and D. G. Capone (2004), High rates of N_2 fixation by unicellular diazotrophs in the oligotrophic Pacific Ocean, *Nature*, *430*(7003), 1027–1031, doi:10.1038/nature02824.

Moore, J. K., and O. Braucher (2008), Sedimentary and mineral dust sources of dissolved iron to the world ocean, *Biogeosciences*, *5*, 631–656.

Moore, J. K., and S. C. Doney (2007), Iron availability limits the ocean nitrogen inventory stabilizing feedbacks between marine denitrification and nitrogen-fixation, *Global Biogeochem. Cycles*, *21*, GB2001, doi:10.1029/2006GB002762.

Moore, J. K., S. C. Doney, J. C. Kleypas, D. M. Glover, and I. Y. Fung (2001), An intermediate complexity marine ecosystem model for the global domain, *Deep Sea Res., Part II*, *49*, 403–462, doi:10.1016/S0967-0645(01)00108-4.

Moore, J. K., S. C. Doney, and K. Lindsay (2004), Upper ocean ecosystem dynamics and iron cycling in a global three-dimensional model, *Global Biogeochem. Cycles*, *18*, GB4028, doi:10.1029/2004GB002220.

Moore, J. K., S. C. Doney, K. Lindsay, N. Mahowald, and A. F. Michaels (2006), Nitrogen-fixation amplifies the ocean biogeochemical response to decadal timescale variations in mineral dust deposition, *Tellus, Ser. B*, *58*, 560–572, doi:10.1111/j.1600-0889.2006.00209.x.

Parekh, P., M. J. Follows, and E. A. Boyle (2005), Decoupling of iron and phosphate in the global ocean, *Global Biogeochem. Cycles*, *19*, GB2020, doi:10.1029/2004GB002280.

Pehkonen, S. O., R. Siefert, Y. Erel, S. Webb, and M. R. Hoffman (1993), Photoreduction of iron oxyhydroxides in the presence of important atmospheric organic compounds, *Environ. Sci. Technol.*, *27*, 2056–2062, doi:10.1021/es00047a010.

Sabine, C. L., and R. A. Feely (2007), The oceanic sink for carbon dioxide, in *Greenhouse Gas Sinks*, edited by D. Reay et al., pp. 31–49, CABI Publ., Oxfordshire, U. K.

Sarmiento, J. L., and C. Le Quéré (1996), Oceanic carbon dioxide uptake in a model of century-scale global warming, *Science*, *274*, 1346–1350, doi:10.1126/science.274.5291.1346.

Sarmiento, J. L., T. M. C. Hughes, R. J. Stouffer, and S. Manabe (1998), Simulated response of the ocean carbon cycle to anthropogenic climate warming, *Nature*, *393*(6682), 245–249, doi:10.1038/30455.

Schroth, A. W., J. Crusius, E. R. Sholkovitz, and B. C. Bostick (2009), Iron solubility driven by speciation in dust sources to the ocean, *Nature Geosci. Lett.*, doi:10.1038/NGEO501.

Sedwick, P. N., T. M. Church, A. R. Bowie, C. M. Marsay, S. J. Ussher, K. M. Achilles, P. J. Lethaby, R. J. Johnson, M. M. Sarin, and D. J. McGillicuddy (2005), Iron in the Sargasso Sea (Bermuda Atlantic Time-series Study region) during summer: Eolian imprint, spatiotemporal variability, and ecological implications, *Global Biogeochem. Cycles*, *19*, GB4006, doi:10.1029/2004GB002445.

Sedwick, P., E. R. Sholkovitz, and T. M. Church (2007), Impact of anthropogenic combustion emissions on the fractional solubility of aerosol iron: Evidence from the Sargasso Sea, *Geochem. Geophys. Geosyst.*, *8*, Q10Q06, doi:10.1029/2007GC001586.

Siefert, R. L., S. O. Pehkonen, Y. Erel, and M. R. Hoffman (1994), Iron photochemistry of aqueous suspensions of ambient aerosol with added organic acids, *Geochim. Cosmochim. Acta*, *58*, 3271–3279, doi:10.1016/0016-7037(94)90055-8.

Siefert, R. L., A. M. Johansen, M. R. Hoffmann, and S. O. Pehkonen (1997), Measurements of trace metal (Fe, Cu, Mn, Cr) oxidation states in fog and stratus clouds, *J. Air Waste Manage. Assoc.*, *48*, 128–143.

Siefert, R. L., A. M. Johansen, and M. R. Hoffman (1999), Chemical characterization of ambient aerosol collected during the southwest monsoon and intermonsoon seasons over the Arabian Sea: Labile-Fe(II) and other trace metals, *J. Geophys. Res.*, *104*, 3511–3526, doi:10.1029/1998JD100067.

Spokes, L. J., T. D. Jickells, and B. Lim (1994), Solubilisation of aerosol trace metals by cloud processing: A laboratory study, *Geochim. Cosmochim. Acta*, *58*, 3281–3287, doi:10.1016/0016-7037(94)90056-6.

Tegen, I., M. Werner, S. P. Harrison, and K. E. Kohfeld (2004), Relative importance of climate and land use in determining present and future global soil dust emission, *Geophys. Res. Lett.*, *31*, L05105, doi:10.1029/2003GL019216.

U.S. Department of Commerce (2006), 2-minute global gridded relief data, Natl. Oceanogr. and Atmos. Admin., Natl. Geophys. Data Cent., Silver Spring, Md.

Werner, M., et al. (2002), Seasonal and interannual variability of the mineral dust cycle under present and glacial climate conditions, *J. Geophys. Res.*, *107*(D24), 4744, doi:10.1029/2002JD002365.

Woodward, S., D. L. Roberts, and R. A. Betts (2005), A simulation of the effect of climate change-induced desertification on mineral dust aerosol, *Geophys. Res. Lett.*, *32*, L18810, doi:10.1029/2005GL023482.

Wu, J., et al. (2007), Dissolution of aerosol iron in the surface waters of the North Pacific and North Atlantic oceans as determined by a semi-continuous flow-through reactor method, *Global Biogeochem. Cycles*, *21*, GB4010, doi:10.1029/2006GB002851.

Yeager, S. G., W. G. Large, J. J. Hack, and C. A. Shields (2006), The low-resolution CCSM3, *J. Clim.*, *19*(11), 2545–2566, doi:10.1175/JCLI3744.1.

Zhuang, G., Z. Yi, R. A. Duce, and P. R. Brown (1992), Link between iron and sulphur cycles suggested by detection of Fe(II) in remote marine aerosols, *Nature*, *355*, 537–539, doi:10.1038/355537a0.

S. C. Doney, Department of Marine Chemistry and Geochemistry, Woods Hole Oceanographic Institution, Woods Hole, MA 02543-1543, USA.

A. Krishnamurthy, J. K. Moore, and C. S. Zender, Earth System Science, University of California, Irvine, CA 92697, USA. (aparnak@uci.edu)

K. Lindsay, Climate and Global Dynamics Division, National Center for Atmospheric Research, P.O. Box 3000, Boulder, CO 80307, USA.

C. Luo and N. Mahowald, Earth and Atmospheric Sciences, Cornell University, Ithaca, NY 14850, USA.